Petroleum Science 19 (2022) 397–408

Contents lists available at ScienceDirect

Petroleum Science

journal homepage: www.keaipublishing.com/en/journals/petroleum-science

Original Paper

Insights into the multiple applications of modified polyacrylamide as oilfield corrosion inhibitor and water phase tackifier

Tong Han [a], Ji-Xiang Guo [a, *], Qing Zhao [b], Tao Shen [b], Shi-Ling Zhang [a]

[a] Unconventional Natural Gas Institute, China University of Petroleum, Changping, Beijing, 102249, People's Republic of China
[b] State Key Laboratory of Heavy Oil Processing and College of Science, China University of Petroleum, Changping, Beijing, 102249, People's Republic of China

ARTICLE INFO

Article history:
Received 14 May 2021
Accepted 26 September 2021
Available online 13 January 2022

Edited by Xiu-Qiu Peng

Keywords:
Corrosion inhibitor
Polymer
Multifunctional pharmacy
Computational study

ABSTRACT

In order to obtain a multifunctional oilfield agent with both corrosion inhibition and oil displacement functions, a polymer with benzene ring structures is synthesized based on polyacrylamide (PAM) and used as inhibitor for the first time. Methods including electrochemistry, weight loss and theoretical calculations are used to study the inhibition effect for P110 steel in 1.0 M HCl. The experimental results show that the modified polymer poly-(Z)-N-benzylidenepropionamide (PBAM) has excellent inhibition effects, and the maximum efficiency can reach 90.62% in impedance spectroscopy tests. The benzene ring structure added in the modified polymer provides π electrons for the adsorption of inhibitor on metal surface, strengthens the adsorption, and thus brings a better corrosion inhibition effect. In addition to the corrosion inhibition performance, the viscosity-increasing effect of PBAM is evaluated. The results show that the addition of benzene ring not only enhances the corrosion inhibition effect, but also brings temperature resistance to the polymer. However, the salt tolerance of the polymer is affected, the synthesized PBAM which viscosity can above 500 mPa s at 140 °C is suitable for high temperature and low salinity environment. The modified polyacrylamide has satisfactory corrosion inhibition and oil displacement performance, which provides a new idea for the development of oilfield chemistry.

1. Introduction

Petroleum, as a very important strategic energy source, every aspect of its exploitation process is vital. In the process of oilfield exploitation, due to factors such as the downhole environment and acid injection production, the wellbore and oil pipeline will be corroded to varying degrees. Corrosion can cause rapid failure of metal pipelines and equipment, causing serious economic losses and production safety risks (Ma et al., 2020; Mand and Enning, 2020). In order to deal with the corrosion problem in the oil field, the researchers chose many solutions, including corrosion inhibitors, new materials, coatings and so on (Chang et al., 2012; Grachev et al., 2020; Liao et al., 2018; Raps et al., 2009; Rosliza et al., 2011). Among them, corrosion inhibitors are widely used in downhole corrosion inhibition operations due to their advantages of simple operation and low cost. In oilfield development, corrosion inhibitors are needed to protect equipment and pipelines during many processes, such as acid fracturing, wellbore lifting, and crude oil transportation. For organic molecules, if there are N, S, O or other heteroatoms or ring structures in molecular structures, then these organic molecules have the possibility of becoming corrosion inhibitors (Wang et al., 2010). At present, some polymers have been tried for corrosion protection of metals due to their heteroatom functional groups (Atta et al. 2011; Biswas et al., 2015; Cui et al., 2019). In the current research on the use of polymers as anti-corrosion, a considerable part of them uses biological materials such as chitosan. Although biological macromolecules can play a very good role in inhibiting corrosion, their sources limit their large-scale application in oil fields, and polymers that can already be produced in low-cost industrial production have advantages in this regard. In addition, compared with synthetic polymers, biological macromolecules are easier to decompose or fail in the complex environment of oil fields, which is another important reason for the limited use of macromolecular corrosion inhibitors in oil fields.

In the process of crude oil extraction, in addition to preventing corrosion of equipment and pipelines. Enhanced oil recovery (EOR)

* Corresponding author.
E-mail address: guojixiang@cup.edu.cn (J.-X. Guo).

https://doi.org/10.1016/j.petsci.2022.01.003

Abbreviations and symbols

Abbreviations

PAM	polyacrylamide;
PBAM	poly-(Z)-N-benzylidenepropionamide
EOR	enhanced oil recovery
SEM	scanning electron microscope
EDS	element distribution scanning system
DFT	density functional theory
GGA	generalized gradient approximation
BLYP	the correlation function set of Becke-Lee-Yang-Parr
HOMO	highest occupied molecular orbital
LUMO	lowest unoccupied molecular orbital

5.2 Symbols

C	concentration, mg/L
i	corrosion current density, mA/cm^{-2}
b_c	cathode slope, V/dec
b_a	anode slope, V/dec
E_{corr}	corrosion potential, V
η	efficiency, %
R_s	solution resistance, Ω
R_{ct}	charge transfer resistance, Ω
Q	phase angle element
C_{dl}	electric double layer capacitance, μF/cm^2
V_{corr}	corrosion rate, mm/y
R	gas constant, 8.314 J/mol·K
T	absolute temperature, K
M	relative molecular mass
ΔG	Gibbs free energy, kJ/mol
E_{HOMO}	energy of highest occupied molecular orbital, eV
E_{LUMO}	energy of lowest unoccupied molecular orbital, eV
E_A	electron affinity; I:ionization potential
ΔN	electrons fraction

after water injection development is also an important part of increasing crude oil production. After the water injection production enters the middle and late stages, the water content of the oil well will become higher and higher, and the output will drop rapidly. In this case, further improving oil recovery is an important task that oil workers must undertake, and it is also a challenge that oilfield development has been facing (Guo et al., 2021). In conventional methods of EOR, polymer flooding technique belongs to a very efficient technique, this technique has the advantage of low cost of raw materials and simple actual production (Zhen et al., 2011). The mainly method of polymer flooding is injecting high molecular weight polymer into water, increase the viscosity of water, which can improve the oil displacement efficiency. The schematic diagram of polymer flooding is shown in Fig. 1. Polymer flooding technology has a history of at least 50 years, among which the most common polymer used in large-scale applications are HPAM and xanthan (Firozjaii and Saghafi, 2020). In addition, some biopolymers have been synthesized and tested for polymer flooding in recent years, but no large-scale application has been seen (Firozjaii and Moradi, 2018). PAM has the advantages of abundant raw materials, low cost and better effect. It is the most common polymer-driven polymer. However, the application of PAM in high temperature and high salt reservoirs has certain limitations. Xanthan gum is another polymer flooding agent that is currently widely used, but there are fewer reports of xanthan gum compared to PAM (Huh and Pope, 2008). Generally speaking, xanthan gum is more resistant to temperature and salinity than PAM, so xanthan gum will show better performance at lower temperature salinity. However, under high temperature and high salinity, xanthan gum will also suffer degradation problems (Kamal et al., 2015). In addition, the higher cost of xanthan gum compared to PAM and the prone to breeding of microorganisms further limit its larger-scale application. In order to improve the temperature and salt resistance of polymers, a common method is to add small amount of crosslinking agent to make the polymer form weak crosslinking system that is hard to be degraded. At present, the main application of polymers, especially PAM, in oilfields is still concentrated in enhanced oil recovery technology, and there are few researches on the application of PAM in other oilfield chemistry fields.

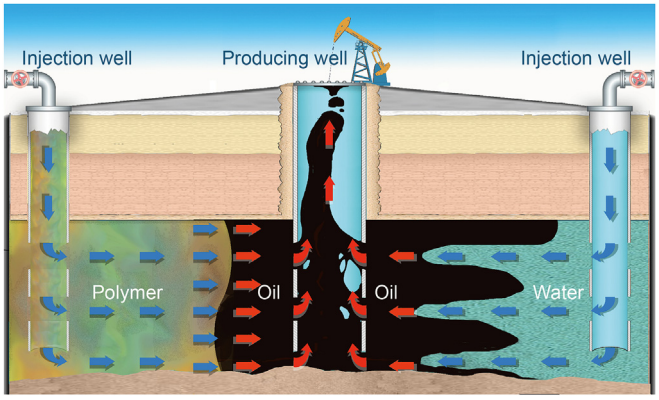

Fig. 1. The schematic diagram of polymer flooding.

In oilfield production, there are already corrosion inhibitors and viscosifiers that have achieved industrial applications. However, in recent years, many oil fields have put forward the research and development needs of multifunctional agents. Multifunctional agents can have different effects such as oil displacement, emulsification, corrosion inhibition, etc. according to the amount and usage conditions. The use of multifunctional agents in oilfield can reduce the storage and transportation costs caused by the use of multiple agents and simplify the operation process. Multifunctional agents can provide positive significance for improving the economic efficiency of oilfield development. In this study, polyacrylamide is modified, and a derivative of PAM, PBAM, is obtained. The chemical structure is shown in Fig. 2. PBAM is synthesized for the first time in this study. This molecule introduces a Schiff base group in polymer chain, polymer has a promoting effect on increasing the viscosity of the water phase, and the Schiff base has been proven to be used for corrosion protection. These two structures are placed in molecule at the same time, which is to make the product have both characteristics of these two groups. The corrosion inhibition effect of polymers on P110 steel in hydrochloric acid is tested. Testing methods include electrochemical method, weightlessness method, surface analysis, etc. After that, quantum chemistry is used to study the corrosion inhibition mechanism of PAM and PBAM. In addition, the viscosity-increasing effect of the polymer on water before and after the modification is tested. This research expands new research directions for polymer flooding and also provides new ideas for oilfield corrosion protection.

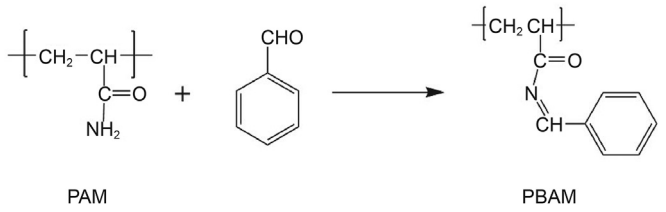

Fig. 2. The chemical structure and modification process of PBAM.

2. Material and methods

2.1. Material

In the corrosion experiment, 1.0 M HCl is selected as the corrosion medium, and 37% wt concentrated hydrochloric acid is used to prepare the corrosion solution. In all experiments, the corrosion temperature is set to 30 °C. The material used for corrosion is P110 steel, and the composition of this material is given in the supply materials (Table S1). Before experiments, the surface of the steel is cleaned with petroleum ether, and then cleaned with ethanol and deionized water. The cleaned sample is dried in a nitrogen environment for later use (Liao et al. 2016, 2017). The PAM used for corrosion inhibitor synthetic is AR grade, and the molecular weight is about 5 million. In synthesis experiment, certain quality of PAM is weighted and slowly added to distilled water under stirring conditions. After PAM is completely dissolved, the solution is stand for 24 h. After that, the benzaldehyde is weighed out according to the set proportion and dissolved in small amount of ethanol, and then this solution is slowly added to PAM solution under stirring conditions. The reaction is carried out at 80 °C for 12 h under a nitrogen atmosphere. After reaction, part of the solvent is distilled under reduced pressure, and the remaining reactant are dried and pulverized in a vacuum freeze dryer to obtain the synthetic product PBAM. The structure of PAM and PBAM is characterized by infrared spectroscopy to confirm that the synthesis reaction has been successfully carried out. The detailed test results of the infrared spectroscopy are given in the supply materials (Fig. S1).

In the viscosity test experiment, in order to evaluate the salt resistance of the polymer, simulated water is prepared according to the on-site formation water of an oil field in Xinjiang, China. The preparation method of the simulated water is as follows: weight 38.02 g $CaCl_2$, 3.10 g $MgCl_2$, 0.81 g KCl, 0.14 g Na_2SO_4, 0.13 g $NaHCO_3$ and 197.29 g NaCl with a balance. After that, these mixtures are dissolved with deionized water and prepared to 1 L solution. When testing the effect of salinity on gelation, the formation water is diluted according to the required salinity. In order to prepare the polymer glue used for polymer flooding, the polymer of the corresponding quality needs to be weighed according to the required concentration before the test, added to the simulated formation water or deionized water and fully stirred for 2 h, sealed and matured for 24 h to make a base fluid for later use (Wang et al., 2011).

2.2. Corrosion inhibition measurements

2.2.1. Electrochemical tests

The electrochemical tests of polymer's corrosion inhibition performance include potentiodynamic polarization curves (Tafel curves) and impedance spectroscopy. All tests are carried out in a flat corrosion electrolytic cell. The instrument is CHI660E electrochemical workstation, and the test system is a working electrode-reference electrode-counter electrode system composed of P110 specimen-Ag/AgCl-platinum sheet (Cui et al., 2019; Sedik et al., 2020). Before the test, samples are immersed in the corrosive solution for at least 1 h to ensure that the open circuit potential (OCP) of the system is stable, and then corresponding tests are carried out (Abd-Elaal et al., 2017). The scanning range of Tafel curve experiments are determined to be 0.5 V on the left and right sides of the OCP, and the scanning rate is 0.1 V/s. In the impedance test, the AC frequency range is 200,000–0.1 Hz, and the amplitude is 10 mV around OCP (Salarvand et al., 2017). In order to ensure the accuracy of the results, each group of experiments carry out three parallel experiments, after confirming that there is no obvious error between the parallel experiments, data analyzing will be carried out. All test results are analyzed after fitting processing using corresponding software.

2.2.2. wt loss method

In weight loss experiments, the processed samples are immersed in different concentrations of corrosion inhibitor solutions for 72 h (Umoren et al., 2015). After that, the corrosion products on the surface of samples are cleaned, then remaining mass of the samples are weighted (Mobin et al., 2017). The corrosion rate and corrosion inhibition efficacies are calculated, equations which are used can be found in supply materials (Eq. (S1) and Eq. (S2)) (Gao et al., 2009). All experiments are repeated three times, and the results are averaged to reduce possible errors. After obtaining the static weight loss results, in order to further evaluate the corrosion inhibition performance of PBAM, dynamic corrosion evaluation is carried out. The samples used included P110S, 20# and 316L in addition to P110.

2.2.3. Scanning electron microscope (SEM) study

In order to analyze the influence of the corrosion inhibitor on the surface of P110 sample, Qunta 200F scanning electron microscope is used to test the surface morphology of the steel specimen before and after corrosion. Before the test, all samples are immersed in different corrosive media (corrosion inhibitor concentration is 500 mg/L) for three days and dried in a nitrogen environment. After scanning the surface morphology, the element distribution on the metal surface is obtained through element distribution scanning system (EDS) (Cui et al., 2019).

2.3. Computational studies

In order to explain the mechanism of corrosion inhibitor from the perspective of molecular structure, theoretical calculations are carried out on the molecular structure, electronic arrangement and adsorption of the corrosion inhibitor on the iron surface. Materials Studio software is used for calculation. In the calculation, because the actual polymer is a super-large molecule with repeating units, in order to simplify the calculation, the structural units of PAM and PBAM are used for molecular simulation. In the process of molecular structure simulation, the calculation is completed based on density functional theory (DFT), and the module used is DMol3. DFT theory expresses the kinetic energy of an atom as a functional of electron density, and adds the classical expressions of nucleus-electron and electron-electron interaction (both effects can be expressed by electron density) to calculate the energy of the atoms. All calculations are performed using the generalized gradient approximation (GGA) and the correlation function set of Becke-Lee-Yang-Parr (BLYP) (Liao et al., 2018). The calculation type is Geometry Optimization, and the calculation includes Density of states, Frequency and Orbitals.

After obtaining the optimized structure of the polymer structural units, the Fe (110) surface is established, and the adsorption process of the polymer units on the surface is simulated. In order to

provide sufficient depth for the simulated structure and ensure that only non-bonded interactions occur between organic molecules and surface iron atoms, the number of iron atoms layers is set to 5. The calculation process uses the adsorption locator module, and the forcefield is universal forcefield (Raghavendra, 2020).

2.4. Viscosity test of polymers for flooding

In the viscosity test experiment, the additive amount of polymer is 0.5% wt. In the polymer temperature resistance test, take the mature polymer base liquid prepared with deionized water, add 0.1% stabilizer and cross-linking agent, stir it thoroughly complete dissolved and pour it into ampoule bottles. These ampoule bottles are placed in ovens at different temperatures after being vacuum treated (Guo et al., 2021). The cross-linking reaction is carried out in ampoule bottles. After gelatinized, gels are taken out and the apparent viscosity of the system is tested with a HAAKE MARSIII rheometer. In the polymer salt resistance test, the base liquid is prepared with simulated water of different salinity, and after the same operation, it is placed in an oven at 140 °C to form a gel. After gelation, the apparent viscosity of the system is tested by HAAKE MARSIII, too. All polymers are prepared in three copies at the same time, and parallel experiments are performed to ensure the accuracy of the experimental results. In viscosity tests, the CC26Ti tumbler measuring system is selected for system viscosity determination, the test mode is CR, the speed is 7.2 s^{-1}, the time is 60 s, the measurement point is 10, and the integration time is 3 s;

3. Results and discussions

3.1. Electrochemical studies

3.1.1. Tafel curve analysis

The results of the Tafel curves are shown in Fig. 3. It can be seen from Fig. 3 that no matter whether PAM and its derivatives are added, the shape of the polarization curves have not changed significantly. The stability of the shape of Tafel curves shows that the addition of polymer does not change the reaction mechanism of

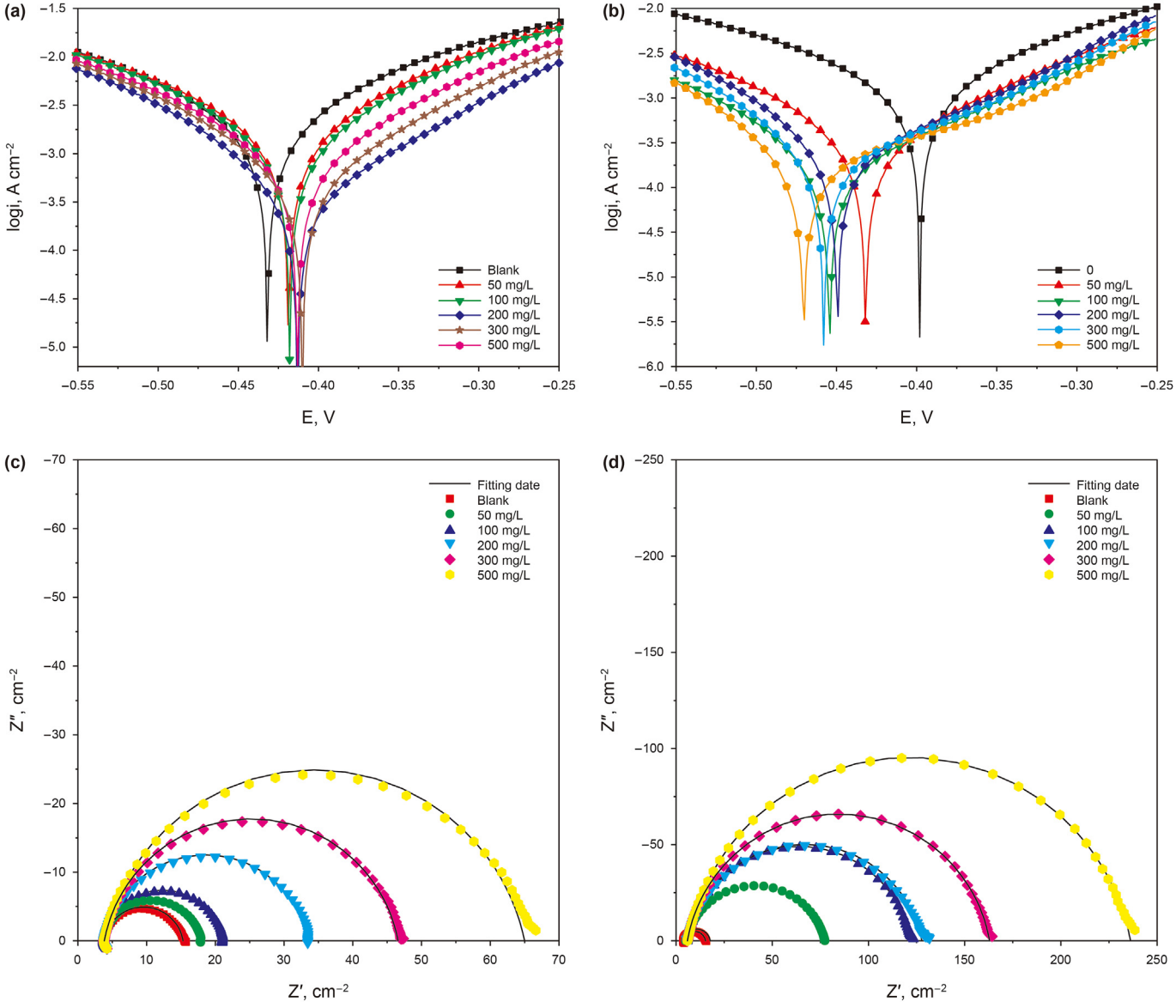

Fig. 3. Electrochemical images of PAM and PBAM (a, b: Tafel curves of PAM & PBAM; c, d: Nyquist plots of PAM & PBAM).

Table 1
Tafel parameters of PAM and PBAM for P110 steel in 1.0 M HCl.

Inhibitors	C (mg/L)	i (mA/cm^{-2})	b_c(V/dec)	b_a (V/dec)	E_{corr}(V vs. SCE)	h (%)
PAM	0	2.351	−0.153	0.150	−0.432	–
	50	1.856	−0.153	0.136	−0.419	21.05
	100	1.508	−0.145	0.128	−0.418	35.86
	200	0.938	−0.132	0.118	−0.413	60.11
	300	0.652	−0.124	0.111	−0.410	72.28
	500	0.446	−0.116	0.106	−0.413	81.02
PBAM	0	2.110	−0.270	0.189	−0.398	–
	50	0.371	−0.134	0.162	−0.432	82.41
	100	0.313	−0.116	0.139	−0.454	85.18
	200	0.289	−0.114	0.126	−0.449	86.28
	300	0.265	−0.112	0.124	−0.458	87.43
	500	0.255	−0.111	0.123	−0.470	87.90

the corrosion reaction (Wang et al., 2011). For PAM, when the concentration is low, the curve does not drop significantly. As the concentration increases, the curve gradually moves downward. The downward shift of Tafel curves mean a decrease in the corrosion current density, and the decrease in this parameter indicates that the corrosion is inhibited (Paul et al., 2019). For PBAM, the corrosion current decreases significantly at a lower addition amount, indicating that the protective performance of modified PAM against hydrochloric acid corrosion may be more satisfactory. In order to quantitatively analyze the Tafel results, the test data is fitted, and various parameters of the curve are obtained and filled in Table 1. The corrosion inhibition efficiency is calculated using the Eq. (S3) in supply materials (Ahmed and Habib 2014).

It can be seen from Table 1 that the corrosion inhibition efficiency of PAM increases as the concentration increases. At 50 mg/L, the corrosion inhibition efficiency is only 21.05%. When the addition amount reaches 500 mg/L, the corrosion inhibition efficiency reaches 81.02%. For PBAM, when the addition amount is 50 mg/L, the efficiency exceeds the efficiency that the 500 mg/L of PAM, and the value is 82.41%. After that, with the gradual increase in the added amount, the efficiency slowly increases, and the efficiency reaches 87.90% at a concentration of 500 mg/L. The obvious increase in corrosion inhibition efficiency shows that the modification does increase the corrosion inhibition performance of polymer molecules.

According to Tafel curve, in addition to get the corrosion current density and efficiency of the corrosion inhibitor at different concentrations, the corrosion potential, cathode and anode slope of the corrosion curve under this condition can be obtained. These two slopes are often used to analyze the effect of corrosion inhibitors (Gao et al., 2009). Table 1 also shows these parameters. Whether PAM or PBAM is added, it can be found that both the cathode slope and anode slope of the corrosion reaction decrease slowly with the increase of the concentration, which shows that the polymer simultaneously inhibits the two processes of metal dissolution and hydrogen evolution in the corrosion reaction (As et al. 2020). Regarding the corrosion potential of the corrosion inhibitor, if the offset of the corrosion potential exceeds 85 mV after adding the corrosion inhibitor, then it can be used as a basis to determine whether the corrosion inhibitor belongs to the cathode type or the anode type(Tourabi et al., 2013; Zulkifli et al., 2017). It can be seen from Table 1 that the maximum potential excursion of PAM is 22 mV, and the maximum excursion of PBAM is 72 mV, neither exceeding the limit of 85 mV. It can be judged from this that, whether modified or not, PAM acts as a mixed corrosion inhibitor for the corrosion of P110 steel in HCl.

3.1.2. Impedance spectroscopy results and analysis

After obtaining impedance test data, Nyquist plots, which always be used for analyzing and describing the experimental results,

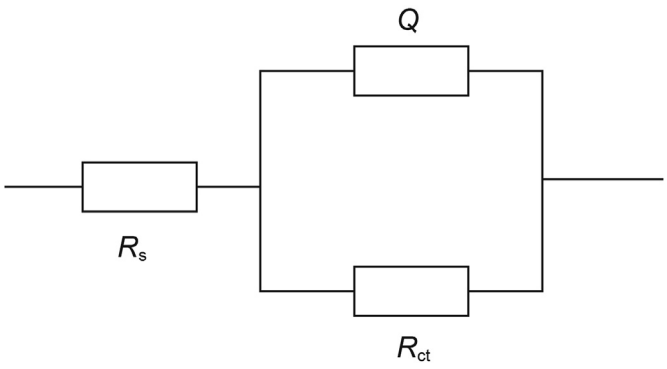

Fig. 4. Circuit used for fitting Nyquist plots.

are fitted and drown from these data (Abdulazeez et al., 2019). The Nyquist plots of PAM and PBAM are shown in Fig. 3. The analog circuit used is given in Fig. 4. From Fig. 3, it can be seen that the Nyquist plots of polymers are not standard semicircular arc shape. The roughness and unevenness of the steel specimen surface may be an important reason for this phenomenon (Nik et al., 2010). As the concentration of corrosion inhibitor increases, the semi-major axis of the impedance arc keeps getting bigger length. The bigger length semi-major axis means that the charge transfer resistance in the corrosion system at this time is greater, which is not conducive to the progress of the corrosion reaction (Yadav et al., 2012). This phenomenon can prove that the two polymers can inhibit the corrosion of metals in solution. For directly perform quantitative analysis on the Nyquist plots, the relevant parameters of the impedance spectrogram are calculated. The calculation results are given in Table 2. The formula used in the calculation is Eq. (S4) and Eq. (S5) in supply materials.

Table 2
Nyquist plots parameters for P110 steel in 1.0 M HCl with PAM and PBAM.

Inhibitors	C(mg/L)	R_s(Ω cm^2)	R_{ct}(Ω cm^2)	C_{dl}(μF/cm^2)	n	η %
PAM	0	3.81	11.55	137.62	0.92	0
	50	3.80	14.01	132.90	0.91	17.56
	100	3.77	17.23	130.12	0.90	32.96
	200	3.84	29.67	124.70	0.91	61.07
	300	3.86	42.93	107.62	0.91	73.09
	500	3.85	61.44	88.90	0.92	81.20
PBAM	0	5.26	21.59	55.98	0.87	0
	50	5.18	72.23	53.09	0.85	70.11
	100	5.85	116.1	47.42	0.89	81.40
	200	5.93	121.8	46.03	0.88	82.27
	300	5.91	157.0	39.87	0.89	86.24
	500	5.98	230.2	29.60	0.88	90.62

In Fig. 4, R_s represents the solution resistance, R_{ct} represents the solution transfer resistance, and Q is a phase angle element. The properties of Q can be determined by the value of n, which is calculated by fitting: the closer n is to 0, the closer the properties of Q are to a complete resistance; on the contrary, the closer to 1, Q will be closer to pure capacitance (Haque et al., 2021). It can be seen from Table 2 that as the concentration increases, the charge transfer resistance of the two polymer systems continues to rise, and finally reaches the maximum when the concentration reaches 500 mg/L (61.44 Ω and 230.2 Ω for PAM and PBAM respectively). At the maximum concentration, the corrosion inhibition efficiency of PAM is 81.20%, while that of PBAM reaches 90.62%. Experimental results show that both polymers can be used as corrosion inhibitors for P110 steel. Further comparing the results, it can be found that no matter from the comparison of charge transfer resistance or efficiency, the corrosion inhibition performance of PBAM is much better than that of PAM, indicating that the modification has a significant effect on the improvement of corrosion inhibition.

In addition to the charge transfer resistance, the electric double layer capacitance (C_{dl}) also decreases with increasing concentration, which is another evidence that the polymer inhibits steel corrosion. Analyzing from the structures of two polymers, for PAM, groups with N atom and O atom in the molecule can provide electrons for the empty orbital of the iron atom on the metal surface, forming adsorption between polymers and metal surface. This process will result in an adsorption film on the metal surface. The existence of this film makes it more difficult for the corrosive medium to contact the iron surface, thereby protecting the metal. However, the strength of this adsorption may be little weaker, so the protection effect is limited. Compared with PAM, PBAM has extra benzene rings in its structure. The benzene ring structure provides more π electrons, resulting in stronger adsorption between PBAM and metal, forming a better protective layer, and showing higher corrosion inhibition efficiency. The results of electrochemical experiments prove that PAM and PBAM can be used as corrosion inhibitors for P110 steel, and at the same time, the PBAM effect obtained after modification is more excellent.

3.2. wt loss method

3.2.1. Corrosion rate and inhibition efficiency

The corrosion rates and corrosion inhibition efficacies obtained in the weight loss experiment are shown in Table 3. It can be clearly seen that in the blank corrosion, the corrosion rate of P110 steel specimen reaches 27.38 mm/y. Such a high corrosion rate means that the steel will corrode rapidly and fail in this environment. When PAM is added, the corrosion rate decreases. When the concentration is 500 mg/L, the corrosion rate decreases to 5.19 mm/y, corresponding to the efficiency of 81.04%. Although PAM can inhibit the corrosion rate of steel, the corrosion rate is still too high and cannot achieve satisfactory results. After adding PBAM, the efficiency can reach 90.21% at 500 mg/L, and the corrosion rate is 2.68 mm/y. Compared with PAM under the same concentration, the corrosion rate is almost reduced by half. The corrosion inhibition effect shown by PBAM is obviously more satisfactory, and it can better protect the steel from corrosion medium.

Table 3
Corrosion rates and inhibition efficiencies of PAM and PBAM.

Inhibitors	Concentration (mg/L)	V_{corr} (mm/y)	η (%)
Blank	0	27.38	–
PAM	50	21.61	21.07
	100	17.55	35.90
	200	10.92	60.12
	300	7.59	72.28
	500	5.19	81.04
PBAM	50	4.32	84.22
	100	3.77	86.23
	200	3.37	87.69
	300	3.09	88.71
	500	2.68	90.21

3.2.2. Dynamic corrosion evaluation of different types of steel

Through electrochemical tests and static weight loss, it has been confirmed that the corrosion inhibition performance of PBAM is significantly stronger than that of PAM. In order to further evaluate the corrosion inhibition ability of PBAM, P110, P110S, 20# and 316L steel samples are used for dynamic corrosion evaluation. The corrosion is carried out in the corrosion reactor, and the stirring speed is 120 r/min. The experimental results are shown in Fig. 5. For P110, P110S and 20# samples, the addition of PBAM can greatly reduce the corrosion rate of hydrochloric acid and reduce the damage of hydrochloric acid corrosion to the samples. For these three samples, the corrosion inhibition rate of PBAM finally reached about 90%. For 316L, the corrosion inhibition rate of PBAM just exceeded 70%, but this does not mean that PBAM is invalid for 316L steel: 316L steel has strong corrosion resistance itself, which can be seen from the far lower blank corrosion rate than other three types. The low rate of blank corrosion caused the corrosion inhibition efficiency of PBAM cannot reach high values. But PBAM can also effectively reduce the corrosion rate of 316L steel. It can be seen from the Fig. 5 that for the four types of samples, PBAM can effectively reduce the dynamic corrosion rate of HCl, indicating that PBAM is an effective corrosion inhibitor, which is consistent with the conclusions obtained in previous experiments.

3.2.3. Adsorption isotherm

Generally speaking, organic corrosion inhibitors adsorb on the metal surface to form an adsorption film which can prevent the damage of the corrosive medium to the surface. Therefore, adsorption isotherms can be used to analyze the interaction between corrosion inhibitors and metal surfaces. The adsorption capacity of the corrosion inhibitor can be described by the surface coverage θ, which is equal to the efficiency of the corrosion inhibitor in value. Through the weight loss test, the efficiency of different concentrations of corrosion inhibitor at 30 °C is obtained. The

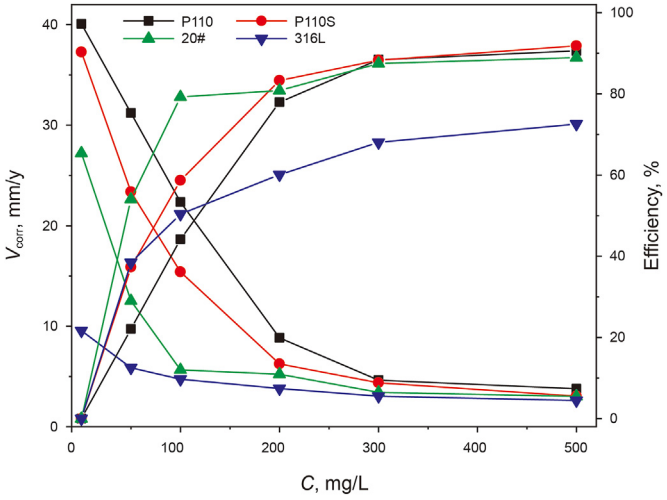

Fig. 5. PBAM dynamic weightlessness experiment results of four different types of steel.

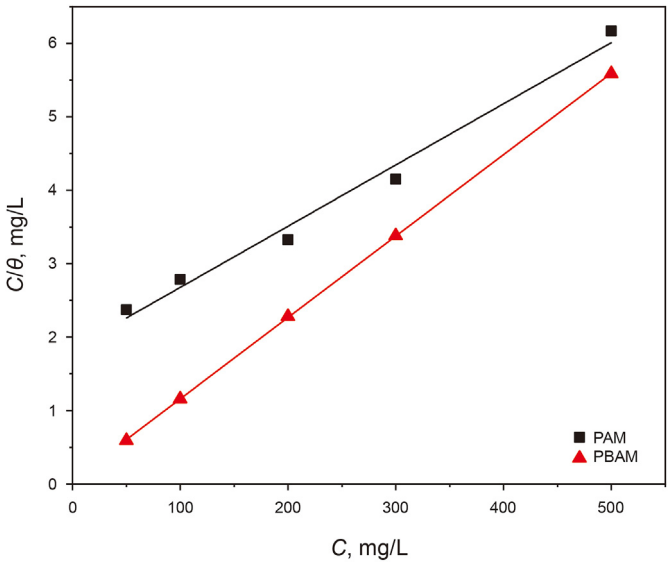

Fig. 6. Langmuir adsorption fitting line of PAM and PBAM.

Table 4
Adsorption process parameters of polymer inhibitors.

Inhibitors	Slope	K_{ads} (L/mg)	R^2	ΔG (kJ/mol)
PAM	0.008	0.542	0.982	−19.39
PBAM	0.011	19.896	0.999	−30.47

Langmuir adsorption isotherm equation is used to fit the data, and the fitting formula is as follows (Shen et al., 2018):

$$C / \theta = 1/K_{ads} + C \quad \text{Eq.(1)}$$

where C represents the inhibitor concentration, K_{ads} is a constant related to the adsorption isotherm equation, which represents the affinity between the surface of steel and organic molecules. K_{ads} can be calculated by the intercept of the fitted line equation (Han et al., 2019). Fig. 6 shows the fitting results of the two polymers, and the relevant parameters are given in Table 4.

Whether it is from the degree of agreement between the original data and the fitted lines or directly based on the correlation coefficient in Table 4 (0.982 and 0.999 for PAM and PBAM, respectively), it can be concluded that the adsorption of PAM and PBAM on P110 surface highly follows the Langmuir adsorption isotherm. The fitting result is close to the Langmuir adsorption isotherm, which means that the adsorption of the two on the P110 steel surface is closer to the single-layer adsorption. It can also be seen from Table 4 that the K_{ads} value of PBAM is higher, which means that the affinity between PBAM and P110 surface is better, which may produce stronger adsorption. After the isotherm fitting parameters are obtained, the Gibbs free energy (ΔG) of adsorption is calculated using following formula:

$$\Delta G = -RT \ln(55.5K_{ads} \times M) \quad \text{Eq.(2)}$$

where R is the gas constant (8.314 J/mol·K), T is the absolute temperature (303 K) and M is the relative molecular mass. Gibbs free energy is an important index to judge the nature of adsorption. When ΔG is less than −40 kJ/mol, the adsorption is considered to be chemical adsorption. At this time, the adsorbent and the adsorbate are connected through the formation of chemical bonds. When ΔG is greater than −20 kJ/mol, only the exchange of electrons between molecules and metal surface takes place. At this time, physical adsorption occurs. When ΔG is between these two values, physical adsorption and chemical adsorption occur simultaneously on the metal surface (Cao et al., 2020). It can be seen from Table 4 that the ΔG of PAM is −19.39 kJ/mol, indicating that PAM only physically adsorbs on the metal surface. The ΔG of PBAM is −30.47 kJ/mol, indicating that PBAM can take place mixed adsorption on P110 surface. Generally, chemical adsorption is stronger than physical adsorption. Both polymers can be physically adsorbed on steel surface, but PBAM additionally occurs chemical adsorption. Therefore, the adsorption effect of PBAM is stronger, the connection with the metal surface is closer, and the metal surface can be better protected from damage. From the analysis of molecular structure, PAM only contains amide groups, and the electrons that can be provided and the degree of freedom of these electrons are very limited, and it is difficult to form a strong interaction with iron atoms. In addition to N and O atoms, PBAM also contains benzene ring structures, which can provide π electrons for adsorption. In the adsorption process, PBAM can interact with the iron surface by π-π interaction, and the strength of this interaction is generally very high, so the adsorption effect of PBAM is stronger than PAM (Cao et al., 2020). Through the fitting and analysis of adsorption isotherms, it can be judged that the adsorption performance of PBAM is better than PAM, and PBAM is more suitable as a corrosion inhibitor for steel. The conclusions obtained from the adsorption isotherm study are consistent with those obtained before.

3.2.4. SEM-EDS microanalyses

In order to study the effect of corrosion inhibitor on the metal surface, SEM is used to obtain the surface micro morphology of the samples treated in different corrosive environments, and the micro photos are shown in Fig. 7. In addition to the microscopic morphology, elemental analysis is also used to analyze the surface elements of P110, and the results are also given in Fig. 7. In Fig. 7 a, a large number of pits and damage caused by corrosion appear on the surface of steel without any corrosion inhibitor. As time increases, this damage will become more and more serious and eventually lead to material failure. In blank corrosion, there are a large amount of chlorine on the surface of the sample. The element chlorine indicates that there is the participation of chloride ions in these destruction processes, and there may be chlorine in the corrosion products of the metal surface. A small amount of oxygen may be related to partial oxidation during sample processing.

In Fig. 7b, compared to Fig. 7a, the damage and pits that can be observed are reduced, but the corrosion of the metal surface is still not optimistic, and a considerable part of the corrosion damage still exists. This phenomenon shows that PAM can only inhibit the corrosion of steel to a certain extent, and the protection effect is not satisfactory. In Fig. 7c, there are almost no corrosion pits visible on the surface of the steel sheet. Instead, there is an approximately layer structure, which may be formed by the adsorption of the PBAM on metal surface. Comparing the microphotographs, it can be inferred that PBAM is more suitable for steel corrosion protection than PAM. Further analyzing the elemental distribution scanning results of the surface, P110 surface treated with PAM and PBAM are compared. In Fig. 7b, the chloride element on the surface of the specimen decreases, the oxygen element has increased, and a small amount of N element has appeared at the same time. It shows that PAM inhibits corrosion damage to a certain extent, and at the same time partially adsorbs on the metal surface. In Fig. 7c, unlike Fig. 7a and Fig. 7b, in the presence of PBAM, the chlorine element is greatly reduced, and the distribution of N element is denser visible. This phenomenon shows that the adsorbed amount of PBAM on the metal surface is more than PAM, effectively inhibiting corrosion damage. SEM-EDS test results show that both PAM and PBAM can

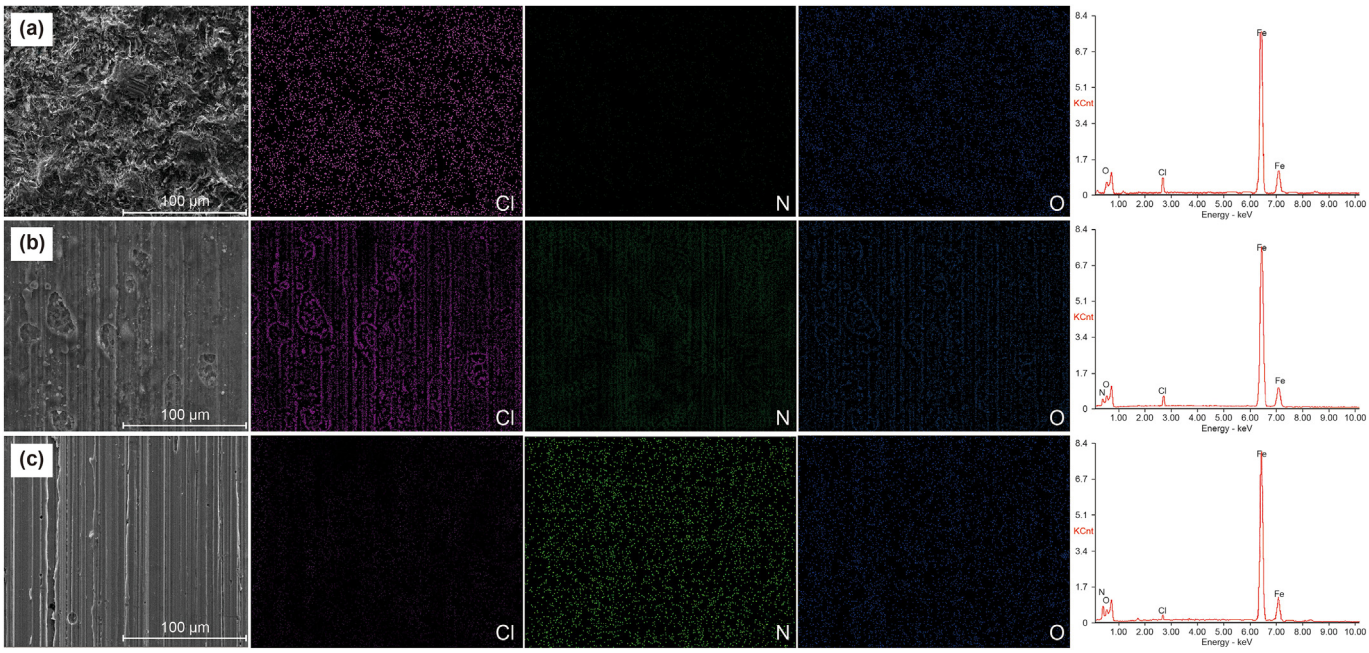

Fig. 7. Microstructure and element distribution on the surface of the sample after corrosion (a: blank corrosion; b: with PAM; c: with PBAM).

reduce the damage occurs on the metal surface, and this protective effect is achieved by the adsorption of organic molecules on the metal surface. PAM can only partially reduce the damage to the metal surface. PBAM has a stronger protective effect than PAM, which is consistent with the previous conclusions.

3.3. Computational chemistry studies

3.3.1. Quantum chemical computation

Generally speaking, organic corrosion inhibitors are adsorbed on the metal surface to form a protective layer to isolate the influence of corrosive substances. This process is affected by the structure of organic molecules. If there are heteroatoms or cyclic structures in the molecule, it is very likely that the molecule can desirable adsorption on metal surface. By calculating the organic molecules and obtaining the relevant data of the molecular frontier orbits, the adsorption performance and corrosion inhibition performance of the molecules on the metal surface can be predicted. Frontier orbitals can be divided into the lowest unoccupied molecular orbital (LUMO) and the highest occupied molecular orbital (HOMO) (Cen et al., 2019). When interacting with the metal surface, the frontier orbitals of the molecule will exchange electrons with the orbitals of the iron atoms. Through density functional theory calculations, the structural units of PAM and PBAM are calculated, and their optimized structure and frontier orbitals are obtained. The obtained structures are shown in Fig. 8. In addition to the orbital structure, the frontier orbital energy and related parameters of the two molecules are also calculated, and the results are shown in Table 5.

After obtaining the orbital energy of the molecule, the electrons fraction ΔN between the organic structure and the iron atom can be obtained by calculation. The data and formula required for the calculation are given in the supporting material (Eq. (S6) to Eq. (S10)). If ΔN is a positive number, then during the adsorption process, the metal will lose electrons and the electrons will be transferred to organic molecules. If ΔN is less than zero, the opposite is true, the metal surface will become an acceptor of electrons from organic molecules (Dutta et al., 2015; Geerlings et al., 2003). It can be seen from the table that the ΔN of PAM and PBAM are 0.948 and 1.249, respectively, which means that when they are combined with the metal surface, they will accept the electrons lost by the iron atoms. As the electron-acquiring party, the LUMO orbitals of organic structures will be used to accept electrons. At this time, PBAM with lower E_{LUMO} may obtain these electrons more easily. It can be predicted that PBAM may have better corrosion inhibition performance. In addition, when ΔN is between 0 and 3.6, organic molecules are considered to be good corrosion inhibitors, and the corrosion inhibition performance becomes better as ΔN increases (Khaled, 2010; Olasunkanmi et al., 2015). Both PAM and PBAM have N in this range. PBAM has ΔN of 1.249, which is higher than PAM. Therefore, the corrosion inhibition performance of PBAM may be even better. Through quantum chemical calculations, it can be concluded that both polymers can be used as corrosion inhibitors, and PBAM may exhibit more satisfactory corrosion inhibition performance, which is consistent with the conclusions obtained from actual experiments.

3.3.2. Adsorption model and energy calculation

In order to simulate the adsorption of the corrosion inhibitor from a microscopic point of view, after obtaining the optimized structure of the corrosion inhibitor molecule, an Fe(110) plane is established to simulate the adsorption of the corrosion inhibitor on the metal surface. The calculated adsorption configuration is shown in Fig. 9. It can be seen from the figure that the organic structures and the metal surface remain approximate parallel. This structure may be due to the relatively uniform distribution of the boundary electrons of the molecules. The relatively flat adsorption of organic structures on the metal surface can provide a great obstacle to the contact between the acidic medium and the metal, and inhibit metal corrosion. Through calculation, the adsorption energy of polymer units is obtained, and the calculation results are given in Table 6.

Adsorption energy includes deformation energy and rigid adsorption energy. The former is the energy released in the process of surface stretching after organic molecules are adsorbed on the metal surface. The rigid adsorption energy is the energy released

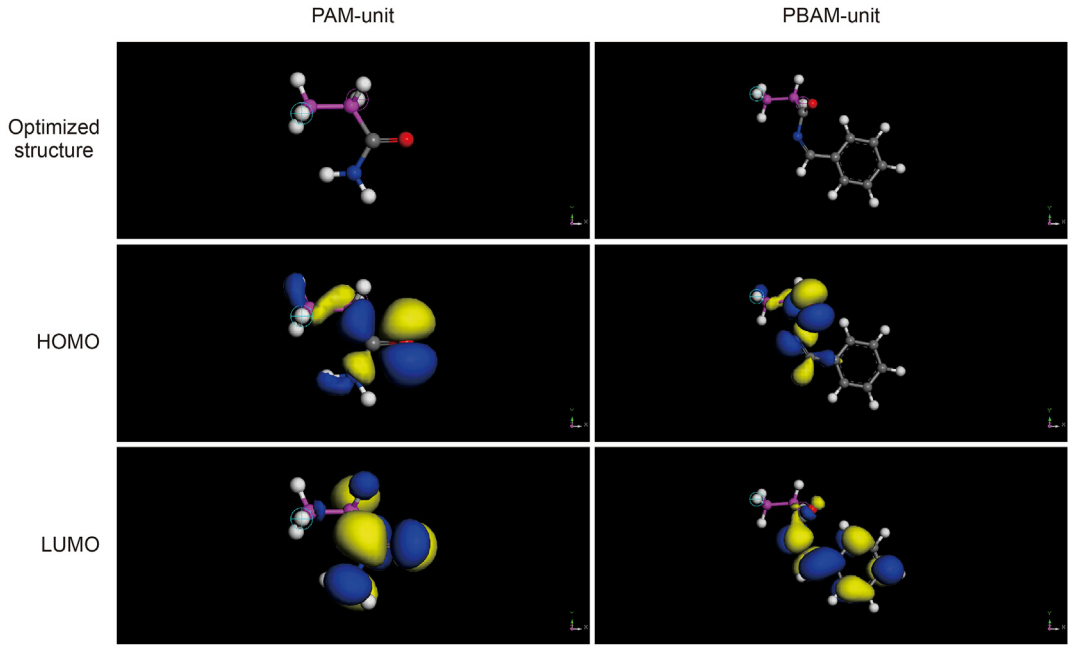

Fig. 8. Optimized structures and frontier orbitals of polymer units.

Table 5
Frontier orbitals parameters of polymer units obtained by calculation.

Molecules	E_{HOMO}(eV)	E_{LUMO}(eV)	I	E_A	χ(eV)	ζ(eV)	ΔN
PAM	−4.687	0.472	4.687	−0.472	2.1075	2.5795	0.948
PBAM	−4.882	−2.054	4.882	2.054	3.468	1.414	1.249

when organic molecules first adsorb on the metal surface (Liao et al., 2018). It should be pointed out that during the simulation, only the structural units of the polymer are studied, and only non-bonding effects are considered. Therefore, the calculated results of adsorption energy only include the physical adsorption part, and the adsorption energy value may be different from the actual situation. In Table 6, the adsorption energies of two structure units are both negative, indicating that the adsorption on the Fe(110) surface releases energy, and it is easy to form a strong adsorption. Comparing the adsorption energy of the two, the adsorption energy of PBAM is higher, which means that the adsorption effect formed by PBAM may be stronger and its potential as a corrosion inhibitor is greater. Quantum calculations are affected by formula models or realistic conditions, and there may be some deviations between the calculation results and the real situation. However, these calculation results can still explain the mechanism and effect of corrosion inhibitors to a certain extent from a theoretical perspective. The conclusions obtained from theoretical calculations and actual experiments both illustrate the potential of polymers as corrosion inhibitors, and at the same time prove that PBAM is a more satisfactory corrosion inhibitor than PAM.

3.4. Viscosity tests of polymers for flooding

3.4.1. Evaluation of temperature resistance

The cross-linked polymer system of PAM and PBAM is configured with deionized water, divided into five equal parts, injected into ampoules, vacuumed, and placed in electric blast drying ovens at different temperatures. After 24 h, the gel conditions results are observed and the viscosity are determined. The viscosity data is used to evaluate the temperature resistance of the polymer gel. The results are shown in Fig. 10a. The viscosity of the PAM increases with the increase of temperature. The main reason is that the higher the reaction temperature, the more violent the molecular movement, and the high temperature promotes the crosslinking reaction. At 140 °C, the viscosity of the polymer is about 250 mPa s. For PBAM, the viscosity of the polymer system increases between 60 °C and 100 °C, and then changes slightly between 100 °C and 140 °C. At 140 °C, the final viscosity can reach more than 500 mPa s. The main reason for the slightly decrease in viscosity at high temperature is that the increase in reaction temperature increases the molecular motion, which promotes the cross-linking reaction and increases the viscosity of the system, but too high temperature will partially degrade the polymer chain and reduce the viscosity. A combination of two factors led to this result. In the temperature resistance test, both PAM and PBAM are weakly cross-linked polymer systems for flooding with good temperature resistance, and the viscosity-increasing effect of PBAM is better than that of PAM. Prior to this study, the author's team had reported this cross-linking system, and the research results showed that the system has good thermal stability (Zhang et al., 2020).

3.4.2. Evaluation of salt tolerance

Take the formation water with different salinity and configure the cross-linked polymer systems to inject them into the ampoules. Then these ampoules are vacuumed and put in an electric heating blast drying box at 140 °C. After 5 days, the gel formation and the viscosity are measured. The result is as follows as shown in Fig. 10b. After 5 days of aging, PAM still has a high viscosity retention rate (viscosity maintained between 200 and 300 mPa s), even in formation water with a salinity of 2.4×10^5 mg/L. It is sure that PAM and has good salt tolerance. However, the viscosity of PBAM decreases rapidly with the increase of the salinity of formation water. After 5 days of aging, it is almost completely hydrolyzed in an environment with a salinity higher than 2.4×10^5 mg/L. The experimental results showed that the modification of PAM improved the temperature resistance of the polymer, but seriously affected the salt resistance of the polymer, the salt tolerance of products is poor. This phenomenon may be due to the fact that the

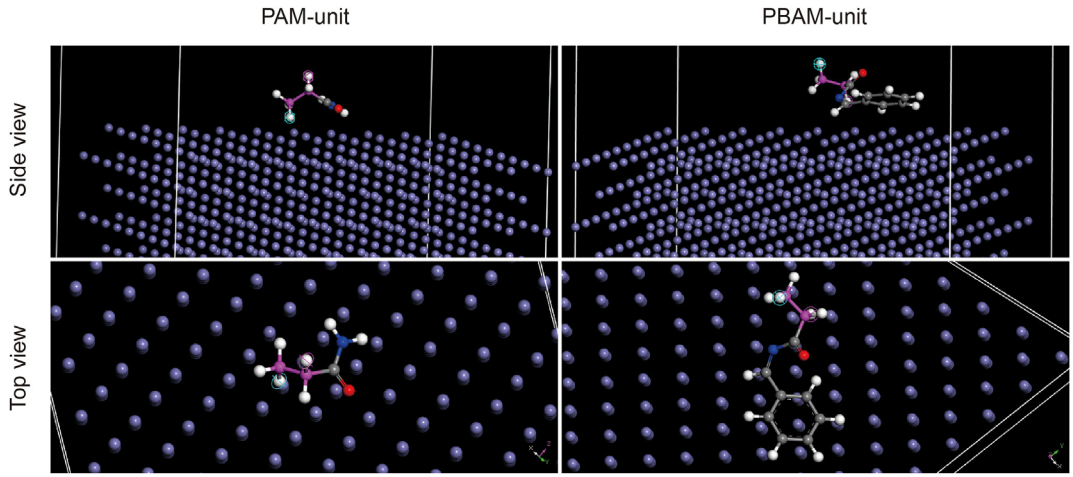

Fig. 9. Adsorption structures of polymer units on Fe (110) surface.

Table 6
Adsorption energy of PAM and PBAM calculated by adsorption simulation.

Molecules	Adsorption energy(kacl/mol)	Rigid adsorption energy(kacl/mol)	Deformation energy (kacl/mol)
PAM	−10.92	−1.67	−9.25
PBAM	−19.67	−3.35	−16.31

rigid structure of the benzene ring increases the temperature resistance during the modification process. However, the synthesis reaction of PBAM is carried out in the water phase, and the polymer may form partially hydrolyzed polyacrylamide during the reaction process, which is prone to carboxyl groups in the gel formation. The carboxyl group is easier to combine with the calcium and magnesium ions in the solution to increase the density of the three-dimensional network structure of the gel, resulting in a structure that has a weaker binding ability to water molecules, and causes the viscosity of the cross-linked system to decrease under high salinity. Viscosity tests results show that both polymers can be used as weak cross-linking viscosity-increasing systems for oil displacement. Among them, PAM has stronger salt tolerance, but its performance at high temperatures is average. PBAM has strong temperature resistance, but it hydrolyzes rapidly under high salinity. Therefore, PBAM may be more suitable for high temperature and low salinity polymer flooding systems, while PAM may be more effective under extreme conditions. The polymer crosslinking viscosity test shows that the modified PBAM can not only be used as a corrosion inhibitor, but also a good temperature-resistant oil displacement system when combined with other agents.

4. Conclusion

In this paper, PAM is modified and a Schiff base based on PAM is synthesized and used as a corrosion inhibitor for the first time. Experimental methods and theoretical calculations are used to study the corrosion inhibition effect of the polymer before and after modification on P110 steel in 1.0 M HCl solution. Weightlessness method, electrochemical test and quantum calculation all show that both polymers can inhibit the corrosion of carbon steel, and the protective effect of modified PBAM is even better. The potentiodynamic polarization results indicate that the polymer corrosion inhibitor is a mixed type corrosion inhibitor. Theoretical

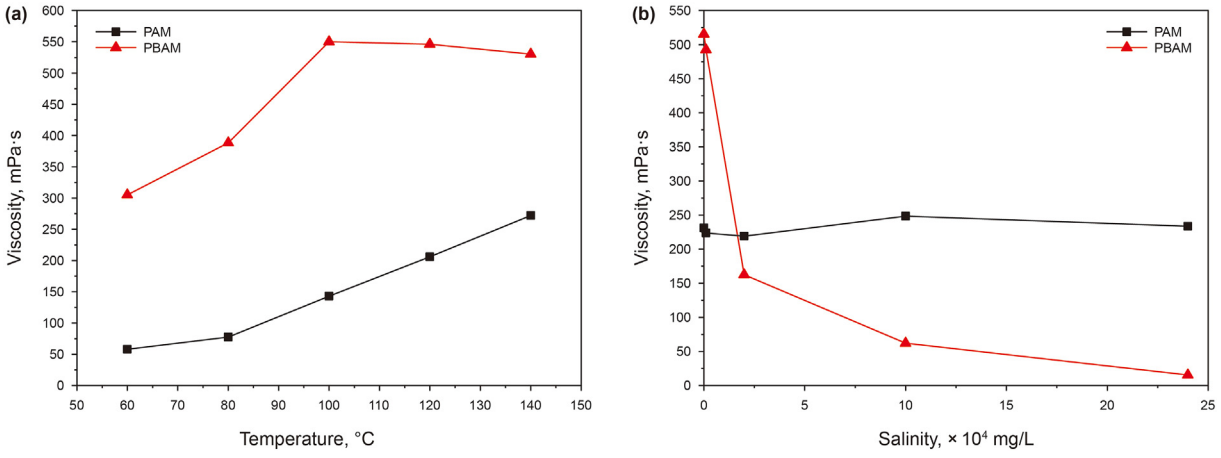

Fig. 10. Polymer viscosity test results (a: temperature resistance; b: salt resistance).

calculations and adsorption isotherms indicate that corrosion inhibitor molecules can exchange electrons with iron and adsorb on the surface of iron. The adsorption behavior of the two polymers conforms to the Langmuir model, in which PAM can only form weak physical adsorption, and PBAM forms mixed adsorption, so the protection effect is stronger. The experimental results show that the benzene ring structure introduced in the polymer provides a π-π interaction that facilitates adsorption and enhances the performance of the corrosion inhibitor. According to the polymer cross-linking viscosity test, the temperature resistance of the modified PBAM is significantly enhanced, but the salt resistance is very weak. It is a high-temperature and low-salinity oil displacement system. In summary, the modified polymer has excellent corrosion inhibition and viscosity-increasing potential at the same time, providing new ideas for the development of oilfield chemistry.

Appendix A. Supplementary data

Supplementary data to this article can be found online at https://doi.org/10.1016/j.petsci.2022.01.003.

References

Abd-Elaal, Ali A., Shaban, Samy M., Tawfik, Salah M., 2017. Three Gemini cationic surfactants based on polyethylene glycol as effective corrosion inhibitor for mild steel in acidic environment. J. Ass. Arab Univ. Basic Appl. Sci. 24 (C), 54–65. https://doi.org/10.1016/j.jaubas.2017.03.004, 2017.

Abdulazeez, I., Khaled, M., Al-Saadi, A.A., 2019. Impact of electron-withdrawing and electron-donating substituents on the corrosion inhibitive properties of benzimidazole derivatives: a quantum chemical study. J. Mol. Struct. 1196, 348–355. https://doi.org/10.1016/j.molstruc.2019.06.082.

Atta AM, El-Azabawy OE, Ismail HS, Hegazy MA. Novel dispersed magnetite core-shell nanogel polymer as corrosion inhibitors for carbon steel in acidic medium. Corrosion Sci.. 201;53(5):1680-1689. doi:10.1016/j.corsci.2011.01.019.

Biswas, A., Pal, S., Udayabhanu, G., 2015. Experimental and theoretical studies of xanthan gum and its graft co-polymer as corrosion inhibitor for mild steel in 15% HCl. Appl. Surf. Sci. 353, 173–183. https://doi.org/10.1016/j.apsusc.2015.06.128.

Cao, G.L., Gao, M.L., Shen, T., Guo, S.X., Zhao, B.B., Zhao, Q., 2020. Asymmetric gemini surfactants modified vermiculite- and silica nanosheets-based adsorbents for removing methyl orange and crystal violet. Colloids Surf. A Physicochem. Eng. Asp. 596, 124735. https://doi.org/10.1016/j.colsurfa.2020.124735.

Cen, H., Cao, J., Chen, Z., Guo, X., 2019. 2-Mercaptobenzothiazole as a corrosion inhibitor for carbon steel in supercritical CO_2-H_2O condition. Appl. Surf. Sci. 476, 422–434. https://doi.org/10.1016/j.apsusc.2019.01.113.

Chang, C.H., Huang, T.C., Peng, C.W., Yeh, T.C., Lu, H.I., Hung, W.I., Weng, C.J., Yang, T.I., Yeh, J.M., 2012. Novel anticorrosion coatings prepared from polyaniline/graphene composites. Carbon 50 (14), 5044–5051. https://doi.org/10.1016/j.carbon.2012.06.043.

Cui, G.D., Guo, J.X., Zhang, Y., Zhao, Q., Fu, S.K., Han, T., Zhang, S.L., Wu, Y.H., 2019. Chitosan oligosaccharide derivatives as green corrosion inhibitors for P110 steel in a carbon-dioxide-saturated chloride solution. Carbohydr. Polym. 203, 386–395. https://doi.org/10.1016/j.carbpol.2018.09.038.

Dutta, A., Saha, S.K., Banerjee, P., Sukul, D., 2015. Correlating electronic structure with corrosion inhibition potentiality of some bis-benzimidazole derivatives for mild steel in hydrochloric acid: combined experimental and theoretical studies. Corrosion Sci. 98, 541–550. https://doi.org/10.1016/j.corsci.2015.05.065.

Firozjaii, A.M., Moradi, S., 2018. Sensitivity analysis and optimization of the effective parameters on ASP flooding compared to polymer flooding using CMG-STARS. J. Petrol Environ. Biotechnol. (1). https://doi.org/10.4172/2157-7463.1000361, 09.

Firozjaii, A.M., Saghafi, H.R., 2020. Review on chemical enhanced oil recovery using polymer flooding: fundamentals, experimental and numerical simulation. Petroleum 6 (2), 115–122. https://doi.org/10.1016/j.petlm.2019.09.003.

Gao, J.C., Weng, Y.J., Salitanate, Feng, L., Yue, H., 2009. Corrosion inhibition of α,β-unsaturated carbonyl compounds on steel in acid medium. Petrol. Sci. 6, 201–207. https://doi.org/10.1007/s12182-009-0032-x.

Geerlings, P., Proft, F.D., Langenaeker, W., 2003. Conceptual density functional theory. Chem. Rev. 103 (29), 793–873. https://doi.org/10.1002/chin.200329289.

Grachev, V.A., Rozen, A.E., Perelygin, Y.P., Kireev, S.Y., Los, I.S., 2020. Multilayer corrosion-resistant material based on iron–carbon alloys. Heliyon 6 (5), e04039. https://doi.org/10.1016/j.heliyon.2020.e04039.

Guo, J.X., Zhang, S.L., Yang, Y.Q., Yu, Z.J., Li, L., Wang, Y.S., Zhang, L.S., 2021. Temperature-resistant and salt-tolerant mixed surfactant system for EOR in the Tahe Oilfield. Petrol. Sci. 18, 667–678. https://doi.org/10.1007/s12182-020-00527-w, 02.

Han, T., Guo, J.X., Zhao, Q., Wu, Y.H., Zhang, Y., 2019. Enhanced corrosion inhibition of carbon steel by pyridyl gemini surfactants with different alkyl chains. Mater. Chem. Phys. 240, 122156. https://doi.org/10.1016/j.matchemphys.2019.122156.

Haque, J., Verma, C., Srivastava, V., Nik, W., 2021. Corrosion inhibition of mild steel in 1M HCl using environmentally benign Thevetia peruviana flower extracts. Sustain. Chem. Pharm. 19, 100354. https://doi.org/10.1016/j.scp.2020.100354.

Huh, C., Pope, G.A., 2008. Residual oil saturation from polymer floods: laboratory measurements and theoretical interpretation. In: Paper Spe Presented at the Spe/doe Improved Oil Recovery Symposium. https://doi.org/10.2118/113417-MS.

Kamal, M.S., Sultan, A.S., Al-Mubaiyedh, U.A., Hussein, I.A., 2015. Review on polymer flooding: Rheology, adsorption, stability, and field applications of various polymer systems. Polym. Rev. 55 (3), 491–530. https://doi.org/10.1080/15583724.2014.982821.

Khaled, K.F., 2010. Experimental, density function theory calculations and molecular dynamics simulations to investigate the adsorption of some thiourea derivatives on iron surface in nitric acid solutions. Appl. Surf. Sci. 256 (22), 6753–6763. https://doi.org/10.1016/j.apsusc.2010.04.085.

Liao, L.L., Mo, S., Lei, J.L., Luo, H.Q., Li, N.B., 2016. Application of a cosmetic additive as an eco-friendly inhibitor for mild steel corrosion in HCl solution. J. Colloid Interface Sci. 474, 68–77. https://doi.org/10.1016/j.jcis.2016.04.015.

Liao, L.L., Mo, S., Lei, J.L., Luo, H.Q., Li, N.B., 2017. Longan seed and peel as environmentally friendly corrosion inhibitor for mild steel in acid solution: experimental and theoretical studies. J. Colloid Interface Sci. 499, 110–119. https://doi.org/10.1016/j.jcis.2017.03.091.

Liao, L.L., Mo, S., Lei, J.L., Luo, H.Q., Li, N.B., 2018. Corrosion protection for mild steel by extract from the waste of lychee fruit in HCl solution: experimental and theoretical studies. J. Colloid Interface Sci. 520, 41–49. https://doi.org/10.1016/j.jcis.2018.02.071.

Ma, Y., Liu, S.T., Zhang, H., Feng, Y.H., Gou, S.C., Bai, H.T., 2020. Study on affecting factors and mechanism of oil Tubing corrosion in Northern shaanxi oil field. Mater. Sci. Forum 977, 108–114. https://doi.org/10.4028/www.scientific.net/MSF.977.108.

Mand, J., Enning, D., 2020. Oil field microorganisms cause highly localized corrosion on chemically inhibited carbon steel. Microb. Biotechnol. 14 (1), 171–185. https://doi.org/10.1111/1751-7915.13644.

Mobin, M., Aslam, R., Aslam, J., 2017. Non toxic biodegradable cationic gemini surfactants as novel corrosion inhibitor for mild steel in hydrochloric acid medium and synergistic effect of sodium salicylate: experimental and theoretical approach. Mater. Chem. Phys. 191, 151–167. https://doi.org/10.1016/j.matchemphys.2017.01.037.

Nik, W., Sulaiman, O., Giap, S., Rosliza, R., 2010. Evaluation of inhibitive action of sodium benzoate on corrosion behaviour of AA6063 in seawater. Int. J. Technol. 1 (1), 20–28. https://doi.org/10.14716/ijtech.v1i1.997.

Olasunkanmi, L.O., Obot, I.B., Kabanda, M.M., Ebenso, E.E., 2015. Some Quinoxalin-6-yl derivatives as corrosion inhibitors for mild steel in hydrochloric acid: experimental and theoretical studies. J. Phys. Chem. C 119 (28), 16004–16019. https://doi.org/10.1021/acs.jpcc.5b03285.

Paul, P.K., Saraswat, V., Yadav, M., 2019. Chromenes as efficient corrosion inhibitor for mild steel in HCl solution. J. Adhes. Sci. Technol. 33 (12), 1–19. https://doi.org/10.1080/01694243.2019.1591774.

Raghavendra, N., 2020. Antifebrin drug prepared via one-stage green method as sustainable corrosion inhibitor for Al in 3 M HCl medium: insight from electrochemical, gasometric, and quantum chemical studies. Surf. Eng. Appl. Electrochem. 56 (2), 235–241. https://doi.org/10.3103/S106837552002012X.

Raps, D., Hack, T., Wehr, J., Zheludkevich, M.L., Bastos, A.C., Ferreira, M.G.S., Nuyken, O., 2009. Electrochemical study of inhibitor-containing organic–inorganic hybrid coatings on AA2024. Corrosion Sci. 51 (5), 1012–1021. https://doi.org/10.1016/j.corsci.2009.02.018.

Rosliza, R., Nik, W.B.W., Izman, S., 2011. Efficiency comparison of some natural products on corrosion inhibition of Al-Mg-Si Alloy. Adv. Mater. Res. 328–330, 1206–1209. https://doi.org/10.4028/www.scientific.net/AMR.328-330.1206.

Salarvand, Z., Amirnasr, M., Talebian, M., Raeissi, K., Meghdadi, S., 2017. Enhanced corrosion resistance of mild steel in 1 M HCl solution by trace amount of 2-phenyl-benzothiazole derivatives: experimental, quantum chemical calculations and molecular dynamics (MD) simulation studies. Corrosion Sci. 114, 133–145. https://doi.org/10.1016/j.corsci.2016.11.002.

Sedik, A., Leran, D., Salci, A., Athmani, S., Bachari, K., Gecibesler, I.H., Solmaz, R., 2020. Dardagan Fruit extract as eco-friendly corrosion inhibitor for mild steel in 1 M HCl: electrochemical and surface morphological studies. J. Taiwan Inst. Chem. Eng. 107, 189–200. https://doi.org/10.1016/j.jtice.2019.12.006.

Shen, T., Gao, M.L., Zang, W.L., Ding, F., Wang, J., 2018. Architecting organo silica nanosheets for regenerable cost-effective organics adsorbents. Chem. Eng. J. 331, 211–220. https://doi.org/10.1016/j.cej.2017.08.084.

Tourabi, M., Nohair, K., Traisnel, M., Jama, C., Bentiss, F., 2013. Electrochemical and XPS studies of the corrosion inhibition of carbon steel in hydrochloric acid pickling solutions by 3,5-bis(2-thienylmethyl)-4-amino-1,2,4-triazole. Corrosion Sci. 75, 123–133. https://doi.org/10.1016/j.corsci.2013.05.023.

Umoren, S.A., Obot, I.B., Madhankumar, A., Gasem, Z.M., 2015. Performance evaluation of pectin as ecofriendly corrosion inhibitor for X60 pipeline steel in acid medium: experimental and theoretical approaches. Carbohydr. Polym. 124, 280–291. https://doi.org/10.1016/j.carbpol.2015.02.036.

Wang, X., Yang, H., Wang, F., 2010. A cationic gemini-surfactant as effective inhibitor for mild steel in HCl solutions. Corrosion Sci. 52 (4), 1268–1276. https://doi.org/10.1016/j.corsci.2009.12.018.

Wang, X., Yang, H., Wang, F., 2011. An investigation of benzimidazole derivative as corrosion inhibitor for mild steel in different concentration HCl solutions.

Corrosion Sci. 53 (1), 113–121. https://doi.org/10.1016/j.corsci.2010.09.029.
Yadav, D.K., Quraishi, M.A., Maiti, B., 2012. Inhibition effect of some benzylidenes on mild steel in 1 M HCl: an experimental and theoretical correlation. Corrosion Sci. 55, 254–266. https://doi.org/10.1016/j.corsci.2011.10.030.
Zhen, Z., Li, J., Zhou, J., 2011. Microscopic roles of "Viscoelasticity" in HPMA polymer flooding for EOR. Transport Porous Media 86 (1), 199–214. https://doi.org/10.1007/s11242-010-9616-6.
Zhang, S.L., Guo, J.X., Gu, Y., Zhao, Q., Yang, Y.Q., 2020. Polyacrylamide gel formed by Cr(III) and phenolic resin for water control in high-temperature reservoirs. J. Petrol. Sci. Eng. 194, 107423. https://doi.org/10.1016/j.petrol.2020.107423.
Zulkifli, F., Ali, N., Yusof, M.S.M., Isa, M.I.N., Yabuki, A., Nik, W.B.W., 2017. Henna leaves extract as a corrosion inhibitor in acrylic resin coating. Prog. Org. Coating 105, 310–319. https://doi.org/10.1016/j.porgcoat.2017.01.017.